Simple transform methods of a force curve obtained by surface force apparatus to the density distribution of a liquid near a surface

AUTHOR(S):

Amano, Ken-ichi; Takahashi, Ohgi

Simple Transform Methods of a Force Curve Obtained by Surface Force Apparatus to the Density Distribution of a Liquid near a Surface

Ken-ichi Amano[a] and Ohgi Takahashi[b]

[a]*Department of Energy and Hydrocarbon Chemistry, Graduate School of Engineering, Kyoto University, Kyoto* 615-8510, *Japan*.

[b]*Faculty of Pharmaceutical Sciences, Tohoku Pharmaceutical University, Sendai* 981-8558, *Japan*.

Author to whom correspondence should be addressed: Ken-ichi Amano.

Electric mail: amano.kenichi.8s@kyoto-u.ac.jp

Abstract

We propose two simple methods that transform a force curve obtained by a surface force apparatus (SFA) into a density distribution of a liquid near a surface of the SFA probe. The transform methods are derived based on the statistical mechanics of simple liquids, where the liquid is an ensemble of small spheres. The solvent species is limited to only one component and two-body potential between the solvent spheres is arbitrary. However, two-body potential between the SFA probe and the solvent is restricted to rigid potential (i.e., the transform methods are derived within the restriction of the rigid potential). In addition, Kirkwood and linear superposition approximations are applied in order to derive the transform methods. The transform methods are simply tested in both hard-sphere fluid and Lennard-Jones (LJ) fluid with hard core potential. The tests are computationally practiced using a three-dimensional integral equation theory. It is found that the transform method with Krikwood superposition approximation (transform method 1) generally reproduces the more precise solvation structure than that with linear superposition approximation (transform method 2). In the test of the hard sphere solvent, it is found that the reproducibility becomes better as the number density of the solvent lower. Furthermore, it is found in the test of the LJ fluid that the reproducibility becomes better as the two-body potential between the SFA probe and the solvent approaches rigid potential. This is because, the transform methods are derived within the model of the rigid potential. It is verified that the transform methods are useful for obtaining of a rough image of the solvation structure. (However, if evaporation or solidification, a phase transition in a local space sandwiched between the two surfaces, occurs while the experiment, the transform methods should not be used.)

Keywords:
Measurement theory
Surface force apparatus
Atomic force microscopy
Solvation structure
Hydration structure

1. Introduction

The surface force apparatus (SFA) has been used to measure the force acting between arbitrary two surfaces in solvents [1,2]. The two surfaces are the force probes for the experiment of SFA, and they can confine various types of the solvents. The force obtained by SFA is usually shown as the *force curve* whose vertical line is force and horizontal line is separation between the two surfaces. In the force curve, there are mainly two origins of the force factors. One is two-body interaction between the two SFA probes themselves, and the other is the solvation force between them. The solvation force is originated from the many-body interaction of the confined solvent particles, and it is the origin of the oscillation in the force curve. In order to understand why the force curve has such an oscillatory shape, several theoretical studies have been performed in the past decades [3-6]. Due to their studies, the mechanism of the oscillatory shape has already been elucidated, however, there is not the method for transforming the force curve obtained with SFA into the (intrinsic) solvation structure on the surface of the SFA probe. In the present study, hence, we propose two transform methods based upon a theory of statistical mechanics of simple liquids. To derive the two transform methods, we take advantage of Kirkwood [7-9] and linear [3] superposition approximations. In this paper, we call the transform method derived by using the Kirkwood superposition approximation and that derived by using liner superposition approximation transform methods 1 and 2, respectively. To test the validity of the both methods, we computationally perform simple tests in both hard sphere fluid and Lennard-Jones (LJ) fluid with hard core potential.

Recently, M. Watkins *et al*. [10] and Amano *et al*. [11] proposed a method for transforming the force distribution measured by atomic force microscopy (AFM) in a solvent [12,13] into the (intrinsic) solvation structure on the solid plate. In the method [10,11], the probe is approximated as a solvent sphere (we call it the ideal probe). This method works well when a solvent sphere or a very similar particle is located on the apex of the probe. Therefore, it has been concluded that a nearly-ideal probe should be used in the real experiment in order to obtain the solvation structure. There have been proposed the simple transform method for AFM to obtain the solvation structure, although the transform method for SFA has not been proposed. This is also the motivation for derivation of the transform methods of SFA. (J. P. Cleveland *et al*. [14] has also proposed a similar equation in AFM study. However, the proposed one is relation between “the potential the AFM probe experiences” and “the position probability of the AFM probe”.)

In the present theory, SFA measurement is simply modeled as shown in Fig. 1. The two cylindrical solids are immersed in the solvent an ensemble of small spheres. (*In theory*, the two solids do not need to be the same, and triangular, rectangular,

pentagonal prisms, and so on can be applied instead of the cylindrical solids.) The solvent species is limited to only one component and two-body potential between solvent spheres is *arbitrary*. However, two-body potential between the SFA probe and the solvent is restricted to rigid potential. A point that should be notified before the derivation of the transform methods is that evaporation and solidification (phase transitions in a local space sandwiched between the two surfaces) are neglected. That is, if the evaporation or solidification occurs in the measurement of the force curve, the force curve must not be used for calculation of the solvation structure.

In the present paper, we particularly explain the derivation process of the transform method 1 (in which Kirkwood superposition approximation is applied) and briefly explain that of the transform method 2 (in which a linear superposition approximation is applied). We obtain the two transform methods starting from a basic equation connecting the solvation force and the solvation structure. (The derivation process of the basic equation is written in Appendix A.) In order to verify the transform methods, simple tests are performed in computer. The tests are conducted in both hard sphere fluid and LJ fluid with hard core potential. In the hard sphere fluid the number density is varied as a parameter, while in the LJ fluid the two-body potential between the SFA probe and the solvent is varied (solvation affinity of the cylindrical solid is varied). As a result, it is found that the transform methods can calculate the rough image of the solvation structure from the solvation force. The accuracies of the transformations are not so high, the reasons of which are originated from introductions of the Kirkwood and linear superposition approximations. However, it is found that the transform method 1 generally reproduces better results in comparison with the transform method 2 (the detailed results of the tests are shown in Chapter 3). In our opinion, the transform method 1 has a potential to become a fundamental method for SFA to obtain the solvation structure. (Recently, some liquid theories [15-18] can calculate the solvation structure very accurately. Thus, one might think that the transform methods here are not valuable methods compared to the liquid theories [15-18]. However, it is not appropriate picture. A different point of the liquid theories and the present transform methods is that the latter can calculate the solvation structure *from* the solvation force obtained by the SFA experiment. That is, the latter is the measurement theory for SFA. Therefore, the former and latter should not be compared directly.)

2. Theory

2.1. Derivations of the transform methods

In this chapter, derivation processes of the transform methods are written. To start

the explanation, we introduce following conditions.

(I) The solvent considered here is a simple liquid, an ensemble of the small spheres. Two-body potential between the solvent spheres is arbitrary.
(II) Cylindrical solids 1 and 2 are immersed in the simple liquid (see Fig. 1). The cylindrical solids have the same shapes and they are rigid bodies. (The cylindrical solid can be alternated with a solid with a plane surface. The examples are triangular, rectangular, pentagonal prisms. Furthermore, the shapes of the solid pair are not required to be the same. For example, the surface areas of the cylindrical solids 1 (sample) and 2 (probe) are not required to be the same. In this study, however, we use the same cylindrical solids in order to simplify the explanation and demonstration of the transform methods.)
(III) The circular surfaces of the cylindrical solids are facing each other, and the circular surfaces are vertical to the z-axis.
(IV) The origin of the whole system is set at the center of the facing surface of cylindrical solid 1 (see the black point in Fig. 1). Cylindrical solid 1 is fixed, whereas cylindrical solid 2 can change its position along the z-axis.
(V) Areas of the circular surfaces are sufficiently large compared to the solvent sphere. (This enables us to ignore complexity of the solvated spheres on the edges of the circular surfaces.)
(VI) The lateral surfaces of the cylindrical solids are horizontal to the z-axis, and hence the solvation force along the z-axis is never generated from the solvated particles on the lateral surfaces.
(VII) The heights of the cylindrical solids are sufficiently tall, so that the solvation structures on the backward surfaces (the non-facing surfaces) are never destroyed during the positional change of the cylindrical solid 2.
(VIII) The evaporation and solidification, phase transitions in a local space sandwiched between the facing surfaces, are ignored in the theory.

From here, we give a description of the derivation process of the transform method 1. (That of the transform method 2 will be simply written afterward.) In the SFA experiment, the force between the two surfaces is measured, and the solvation force can be picked out from the crude force by subtracting the two-body force between the solid surfaces. Its two-body force can be theoretically calculated from the two-body potential or measured by SFA experiment in the air (vacuum). The solvation force along the z-axis being f_{sol} (solvation force acting on the cylindrical solid 2) has a relationship with the number density distribution of the solvated spheres, which is expressed as [3]

$$f_{\mathrm{sol}}(s) = A\int_{-\infty}^{\infty} \rho(z;s)\frac{\partial u_2(z;s)}{\partial z}dz, \tag{1}$$

where A represents the facing surface area of the cylindrical solid 2. $\rho(z;s)$ is the number density of the solvent at z, and s is the separation between the facing surfaces. u_2 is the two-body potential between cylindrical solid 2 and the solvent sphere. If the wall surface area A is infinite, Eq. (1) is exact. In SFA experiment, the sample and probe surfaces are sufficiently large compared with the section area of a solvent molecule. Therefore, Eq. (1) is a reasonable approximation. Eq. (1) is derived by considering an infinitesimal change of the separation between two solids within statistical mechanics of a simple liquid (see Appendix A). Eq. (1) is strictly consistent with the contact theorem [19-21]. (The contact theorem explains the pressure on a wall, the derivation of which is performed by an infinitesimal change of *the volume of a system or a solute*.) To connect the solvation force and the solvation structures on cylindrical solids 1 and 2, we take advantage of the Kirkwood superposition approximation [7-9] and express ρ as

$$\rho(z;s) \approx \rho_0 g_1(z) g_2(z-s). \tag{2}$$

Here, ρ_0 is the bulk number density of the solvent (constant value), and g_i (i = 1 or 2) is a pair correlation function between the cylindrical solid i and solvent. g_i is the so-called a normalized number density of the solvent or a solvation structure around the cylindrical solid i. Applying this approximation, Eq. (1) is rewritten as

$$f_{\mathrm{sol}}(s) = A\rho_0\int_{-\infty}^{\infty} g_1(z) g_2(z-s)\frac{\partial u_2(z-s)}{\partial z}dz. \tag{3}$$

The origin of g_1 is placed at the center of the whole system (see the black point in Fig. 1), whereas the origin of g_2 is placed at the center of the facing circular surface of the cylindrical solid 2 (see the gray point in Fig. 1). The origin of u_2 is the same as that of g_2. Considering the conditions (VI) and (VII), Eq. (3) can be rewritten as

$$f_{\mathrm{sol}}(s) = A\rho_0\int_{0}^{s} g_1(z) g_2(z-s)\frac{\partial u_2(z-s)}{\partial z}dz + A\rho_0\int_{s+w}^{\infty} g_2(z-s)\frac{\partial u_2(z-s)}{\partial z}dz, \tag{4}$$

where w represents the height from the facing surface to the backward surface of the cylindrical solid 2. The two-body potential between cylindrical solid 2 and the solvent sphere being u_2 is expressed as

$u_2 = 0$ for contact points and non-overlapped points, (5a)

$u_2 = \infty$ for overlapped points. (5b)

Then, the value of $\exp[-u_2/(k_B T)]$ is expressed as

$\exp[-u_2/(k_B T)] = 1$ for contact points and non-overlapped points, (6a)

$\exp[-u_2/(k_B T)] = 0$ for overlapped points, (6b)

where k_B and T are the Boltzmann constant and absolute temperature, respectively. Eq. (6) expresses that the $\exp[-u_2/(k_B T)]$ is a step function. Thus, the partial differentiation of u_2 with respect to z can be expressed as

$$\frac{\partial u_2(z-s)}{\partial z} = k_B T \exp[u_2(z-s)/(k_B T)]\{\delta[z-(s-d_S/2)] - \delta[z-(s+w+d_S/2)]\}, \quad (7)$$

where δ and d_S are the delta function and the diameter of the solvent sphere, respectively. By substituting Eq. (7) into Eq.(4), the solvation force acting on cylindrical solid 2 is rewritten as

$$f_{sol}(s) = A k_B T \rho_0 g_1(s - d_S/2) g_2(-d_S/2) - A k_B T \rho_0 g_2(w + d_S/2). \quad (8)$$

Since $-d_S/2$ and $w+d_S/2$ are the contact points between the cylindrical solid 2 and the solvent sphere, the values of $g_2(-d_S/2)$ and $g_2(w+d_S/2)$ both are represented g_C (the subscript C denotes the contact point). Hence, the solvation force is simply rewritten as

$$f_{sol}(s) = A k_B T \rho_0 g_c[g_1(s - d_S/2) - 1]. \quad (9)$$

When $s = d_S$, $g_1(s - d_S/2)$ becomes $g_1(d_S/2)$, and its value is equal to g_C. Therefore, the value of g_C is expressed as

$$g_C = \frac{1}{2} + \frac{\sqrt{A^2 {k_B}^2 T^2 {\rho_0}^2 + 4 A k_B T \rho_0 f_{sol}(d_S)}}{2 A k_B T \rho_0}. \quad (10)$$

In the process of the derivation of Eq. (10), we used the fact that g_C is not equal to 0 but 1 when $f_{sol}(d_S)$ is 0 (see Eq. (9)). This equation implies calculation of the contact number density of the solvent ($\rho_0 g_C$) is possible, when $f_{sol}(d_S)$ is obtained. Subsequently, g_1 can be obtained by the following equation:

$$g_1(s - d_S/2) = \frac{f_{sol}(s)}{Ak_B T\rho_0 g_c} + 1. \quad (11)$$

We call this equation the transform method 1. Here, let us consider the value of g_1 when the solvent sphere is overlapped with the cylindrical solid 1. For example, the value of $g_1(0)$ should be 0, because when the nearest-neighbor distance between the circular surface and the center of the solvent particle is 0 the solvent particle is no longer placed. Hence, now we check this prediction from Eq. (11). When $s-d_S/2=0$, s is equal to $d_S/2$, and $f_{sol}(d_S/2)$ is equal to the solvation force solely from the backward surface f_B (constant). This is because, there are no solvent spheres within the narrow space between the facing surfaces with separation $d_S/2$. The value of f_B is given in the second term of the right-hand side of Eq. (8), which is written as

$$f_B = -Ak_B T\rho_0 g_C. \quad (12)$$

By substituting Eq. (12) into Eq. (11), the value of $g_1(0)$ is calculated to be 0. Consequently, it is proven that the behavior of g_1 at the overlapped region is physically valid. In addition, of course, when the distance between the circular surface and the solvent sphere is long enough, the value of $g_1(s - d_S/2)$ becomes 1, because "$f_{sol}(s) \to 0$" when "$s - d_S/2 \to \infty$".

Next, we briefly explain the transform method 2 in which the linear superposition approximation [3] is applied instead of the Kirkwood one. The linear superposition approximation is expressed as

$$\rho(z; s) \approx \rho_0[g_1(z) + g_2(z - s) - 1\,]. \quad (13)$$

By substituting Eq. (13) into Eq. (1), the following equation is obtained (the detailed derivation process is abbreviated):

$$g_1(s - d_S/2) = \frac{f_{sol}(s)}{Ak_B T\rho_0} + 1. \quad (14)$$

We call this equation the transform method 2. The difference between Eq. (11) and Eq. (14) is only the presence/absence of g_C. Calculation of g_C is not needed in the transform method 2. In the case of Eq. (14), the value of g_1 also becomes 1, when the distance between the circular surface and the solvent sphere is long enough. However, in contrast to Eq. (11), $g_1(0)$ does not become 0 in Eq. (14). Therefore, one can understand that the transform method 1 is physically valid compared with the transform method 2.

2.2. Computational verification of the transform methods

To check the validity of the transform methods, we perform the computational tests. The tests are conducted in both hard sphere fluid and LJ fluid with hard core potential. The tests of the transform methods are done by using liquid theories [22-24], three-dimensional Ornstein-Zernike equation coupled with a hypernetted-chain closure (3D-OZ-HNC) [15]. The grid spacings Δx, Δy, and Δz are set at $0.1d_S$, $0.1d_S$, and $0.02d_S$, respectively. The grid resolution ($N_x \times N_y \times N_z$) is (256×256×2048). It has been verified that the spacing is sufficiently small and the box size ($N_x\Delta x$, $N_y\Delta y$, $N_z\Delta z$) is large enough for the correlation functions at the box surface to be essentially zero. The diameter of the cylindrical solid is set at $10d_S$ [6] and we have checked its diameter is large enough. 3D-OZ-HNC calculates the solvation structure around the cylindrical solid, which acts as a benchmark structure for the solvation structure calculated through the transform methods. Although 3D-OZ-HNC cannot adequately account for the evaporation and solidification of the liquid, the theory is used for the verification of the transform methods. 3D-OZ-HNC is not so very strict, however, it is accurate enough for this first step verification. The transform methods themselves are not derived considering the phase transitions. Hence, if the phase transition occurs in the measurement of the force curve, the transform methods must not be used. The solvation structure calculated only by 3D-OZ-HNC is represented as g_n, where the subscript n represents the normal method. In the normal method, the solvation force between the cylindrical solids is not used, which is different point against the transform methods. Input data for calculation of g_n are as follows: the diameter of the solvent sphere; bulk number density; two-body potential between the solvent-solvent; two-body potential between the solvent-cylindrical solid; and temperature. For hard-sphere fluid, two-body potential between the solvent-solvent is the rigid potential, whereas, for the LJ fluid with hard core potential, it is expressed as

$$\begin{aligned} u_{SS}(r) &= \infty && \text{for} \quad r < d_S, \\ u_{SS}(r) &= -\xi_{SS}(d_S/r)^6 && \text{for} \quad r \geq d_S, \end{aligned} \tag{15}$$

where r is the distance between the centers of the solvent spheres. ξ_{SS} represents the affinity between the solvent-solvent, and $\xi_{SS}/(k_BT)$ is set at 1.5. In Eq. (15), the repulsive part of the 12-6 type potential is replaced by the hard-core interaction, which enables us to determine the contact point between them definitely. In the LJ fluid, the solvation affinity of the cylindrical solid (ξ_{DS}) is varied as a parameter. Two-body potential between the solvent sphere and the cylindrical solid is expressed as [25]

$$u_{DS}(h) = \infty \qquad \text{for} \quad h < d_S/2,$$
$$u_{DS}(h) = -(\xi_{DS}/8)(d_S/h)^3 \exp[-\{h/(10d_S)\}^{10}] \qquad \text{for } h \geq d_S/2, \qquad (16)$$

where h is the distance between the center of the solvent sphere and the nearest surface of the cylindrical solid. The dimensionless value of the solvation affinity being $\xi_{DS}/(k_BT)$ is set at 0.5, 1.0, or 1.5. In Eq. (16), the repulsive part of the 9-3 type potential is replaced by the hard-core interaction, which enables us to determine the contact point between them definitely. The function of $\exp[-\{h/(10d_S)\}^{10}]$ is a moderated step function, which cuts off the long-range interaction [23]. The transform methods requires following input data: the solvation force between the cylindrical solids; surface area of the facing surface of the solid 2; bulk number density; and temperature. Thus, “the normal method” and “the transform methods” are different factures. By the way, it is necessary to prepare the solvation force between the cylindrical solids to perform the test of the transform methods. To prepare it, the solvation structures around a pair of the cylindrical solids 1 and 2 are calculated in various separations. Then, the solvation structures are used for calculation of the curve of the solvation force. Using the transform method, the solvation force curve is transformed into the solvation structure. If the solvation structure is very similar to the solvation structure obtained by the normal method g_n, the transform method turns out to be a good method for estimation of the solvation structure. (One might think Percus-Yecivk closure should be used instead of HNC when the solvent is hard sphere fluid. However, when a solute, i.e. the cylindrical solid is sufficiently large compared with the solvent sphere, HNC should be used.)

3. Results and discussion

3.1. Test of the transform methods in the hard sphere fluid

In what follows, the solvation structures calculated by the normal method (g_n), the transform method 1 (g_{t1}), and the transform method 2 (g_{t2}) are compared. The solvent here is the hard sphere fluid and its number density is a parameter in this survey. If g_{ti} (i = 1 or 2) deviates *little* from g_n, it is concluded that the transform method has worked well. Let us start the comparison among g_n, g_{t1} and g_{t2}. In Fig. 2(a), (b), (c), and (d), dimensionless values of the solvent density being $\rho_0 d_S^3$ are 0.5, 0.6, 0.7, and 0.8, respectively. In appearance, the deviations from g_n becomes smaller as the number density becomes lower. To corroborate the finding, we calculated the surface area of the deviation (S_{dev}) defined as

$$S_{\mathrm{dev}} \equiv \int_{0.5}^{3.5} |g_{ti}(h_n) - g_{\mathrm{n}}(h_n)|\, dh_{\mathrm{n}}, \tag{17}$$

where $h_{\mathrm{n}} = h/d_{\mathrm{S}}$ and $i = 1$ or 2. The values of S_{dev} are displayed in Table 1. The deviation from g_{n} becomes smaller as the distance between the circular surface and the solvent becomes longer. The reproducibility of the transform method 1 is generally better than the transform method 2. Furthermore, unfortunately, minus values are outputted from the transform method 2, the values of which are physically irrelevance.

As the number density becomes higher, the interval between the first solvation layer ($h/d_{\mathrm{S}} = 0.5$) and the second one ($h/d_{\mathrm{S}} \approx 1.5$) is slightly shortened. Although it is difficult to distinguish the intervals of g_{n}, g_{t1} and g_{t2} from Fig. 2, the intervals of g_{t1} and g_{t2} are always shorter than that of g_{n}. This behavior originates from the compression of the solvent during the sandwich. Since the solvent spheres are sandwiched by the two large surfaces, the solvent tends to be compressed. The compression behavior influences on the force curve (an input datum for the transform methods), and therefore the intervals of g_{t1} and g_{t2} are always shorter than that of g_{n}.

3.2. Test of the transform methods in the LJ fluid

The computational verification of the transform methods is conducted also in the LJ fluid. Here, the values of $\rho_0 {d_{\mathrm{S}}}^3$ and $\xi_{\mathrm{SS}}/(k_{\mathrm{B}}T)$ are fixed constant, which are respectively 0.7 and 1.5. The solvation affinity of the cylindrical solid being $\xi_{\mathrm{DS}}/(k_{\mathrm{B}}T)$ is changed as the parameter. In Fig. 3(a), (b), and (c), the values of $\xi_{\mathrm{DS}}/(k_{\mathrm{B}}T)$ are set at 0.5, 1.0, and 1.5, respectively. When the cylindrical solid is solvophobic, the contact number density of the solvent is lower, whereas when it is solvophilic, the contact number density is higher [26,27]. This natural property is also reflected in g_{n}, g_{t1} and g_{t2}. As shown in Fig. 3 and Table 2, the difference between g_{n} and g_{ti} ($i = 1$ or 2) becomes smaller as the solvation affinity becomes smaller. This behavior originates from the theoretical condition (II) that the cylindrical solids are presupposed to be the rigid bodies.

The interval between the first solvation layer ($h/d_{\mathrm{S}} = 0.5$) and the second one ($h/d_{\mathrm{S}} \approx 1.5$) corresponds to the diameter of the solvent sphere (d_{S}). Although it is difficult to distinguish the interval differences among g_{n}, g_{t1} and g_{t2}, the intervals of g_{t1} and g_{t2} are always shorter than that of g_{n}. This behavior comes from the compression of the solvent during the sandwich, too.

4. Conclusions

We have proposed the methods for transforming a force curve measured by SFA into the solvation structure on the surface of the SFA probe. The transform methods have been derived based on the statistical mechanics of the simple liquids, where we have taken advantage of Kirkwood and linear super position approximations to perform the derivations. In the verifications of the transform methods, we have computationally tested them in both the hard sphere fluid and LJ fluid with hard core potential. The verification in the hard sphere fluid has revealed that the transform method 1 always works well compared with that of 2 and the reproducibility becomes better as the number density becomes lower (see Fig. 2 and Table 1). Also in the LJ fluid test (see Fig. 3 and Table 2), it has been found that the transform method 1 always works well compared with that of 2. The reproducibility of the transform method becomes better as the solvation affinity ($\zeta_{DS}/(k_BT)$) becomes lower. This behavior comes from the theoretical condition (II) in which the cylindrical solids are hypothecated to be the rigid bodies. By the way, if the evaporation or solidification occurs during the measurement, the transform method should not be used, because the phase transitions are not considered in the theory. The intervals between the first solvation layer ($h/d_S = 0.5$) and the second one ($h/d_S \approx 1.5$) calculated by the normal method and the transform methods have also been compared. We have found that the intervals of g_{t1} and g_{t2} are shorter than that of g_n. The difference originates from the compression of the solvent during the sandwich. It is deemed that Kirkwood or linear superposition approximation should be improved or a new approach for the transformation should be created in order to decrease the difference. Another cause of the difference between g_n and g_{ti} (i = 1 or 2) is considered to be the use of HNC approximation. The contact theorem is not perfectly satisfied by the integral equation theory with the HNC. This is the additional source for the errors.

In the near future, we will apply the transform method 1 to a real SFA experiment. Recently, Amano and Tanaka derived an improved version of the transform method 1 [28], where the rigid potential between the solvent and the model SFA surface is alternated with a soft attractive potential with hard wall. The improved one is considered to be more practicable. We will show its detailed derivation process and results of its verification tests in the near future. In addition, we will report on the structure of a confined liquid between SFA surfaces. Since the confined liquid structure is related to nanotribology [29], this prospective study including the present transform method could be an important research for its study filed. The present transform methods are derived in a simple liquid, however, it is considered that the transform methods can also be used for calculation of the density distribution of colloid (micell) particles on a surface, if the experimental condition is in an ideal condition [30,31]. Moreover, it can be used for measurement of the wettability of a surface, because the wettability is related to the solvation structure [27]. A recent spectroscopic measurement [32,33] can detect water orientation near a surface.

Meanwhile, our experimental theory can obtain the density distribution near a surface. Thus, it is expected that "water density distribution" and "accompanying water orientations" could be *experimentally* obtained in the future by combining SFA and the spectroscopic measurement.

ACKNOWLEDGEMENTS

We appreciate the discussions with M. Kinoshita, H. Onishi, R. Akiyama, K. Fukami, T. Sakka, N. Nishi, K. Kobayashi and E. Tanaka. This work was supported by the "Foundation of Advanced Technology Institute" and "Joint Usage/Research Program on Zero-Emission Energy Research, Institute of Advanced Energy, Kyoto University (ZE25B-30)."

Appendix A. Relation between solvation force acting on arbitrary two solutes and solvation structure around them

In this chapter, the solvation force acting between two arbitrary solutes is connected with the solvation structure around them, i.e., an original equation for Eq. (1) is derived here. Key points that should be notified here are as follows: (A) the relationship between the solvation force and the solvation structure is derived based on the statistical mechanics of a simple liquid in equilibrium state; (B) the solvation force itself is the partial differentiation of the solvent's free energy with respect to separation between the two solutes. The key point (B) indicates that Eq. (1) contains not only energetic force, but also entropic force, although it is difficult to have an insight into the fact in Eq. (1) at a glance. In the theory, the shape of the solvent molecule is approximated as a small sphere and two-body potential between solvent-solvent is arbitrary. The arbitrary property and the key point (B) enable us to perform the transform methods in both hard-sphere and non-hard-sphere fluids. (The hard-sphere fluid is purely entropic system, whereas the non-hard-sphere fluid contains energy and entropy components in the system.)

When the two solutes are immersed in the solvent, the fundamental partition function Q_0 is expressed as

$$Q_0 = \frac{\zeta^N \zeta_{U1} \zeta_{U2}}{N!} \int \cdots \int \exp\{-\beta U(\mathbf{r}'_{U1}, \mathbf{r}'_{U2}, \mathbf{r}_1, \cdots, \mathbf{r}_N)\} d\mathbf{r}'_{U1} d\mathbf{r}'_{U2} d\mathbf{r}_1 \cdots d\mathbf{r}_N, \quad \text{(A. 1)}$$

where N is the number of small spheres, U the whole system energy, $\mathbf{r}$ three-dimensional position vector. β is equal to $1/(k_B T)$, which is called "inverse

temperature". The subscripts from 1 to N represent the numbers for the solvent particles, and the subscripts U1 and U2 represent solutes 1 and 2, respectively. ζ, ζ_{U1}, ζ_{U2} are expressed as

$$\zeta = \frac{(2\pi m k_B T)^{3/2}}{h^3}, \tag{A.2}$$

$$\zeta_{U1} = \frac{(2\pi m_{U1} k_B T)^{3/2}}{h^3}, \tag{A.3}$$

$$\zeta_{U2} = \frac{(2\pi m_{U2} k_B T)^{3/2}}{h^3}, \tag{A.4}$$

respectively. m, m_{U1}, and m_{U2} represent masses of the solvent particle, solute 1, and solute 2, respectively. h represents Plank's constant. When a system of AFM is considered, the solutes 1 and 2 correspond to the solid plate (sample surface) and the AFM probe, respectively. In the case of SFA, the solutes 1 and 2 both correspond to the solid plates, where one is the sample surface and the other is the SFA probe. In those cases, ζ_{U1} and ζ_{U2} are neglected (i.e., $\zeta_{U1} = \zeta_{U2} = 1$), because the solid plate and probe do not change the positions kinetically. These positions are artificially changed in general. The values of ζ_{U1} and ζ_{U2} are dependent on the situation, however, the conclusion (i.e., Eq. (A.19)) does not change. Thus, it is needless to worry about the values in this study.

When solutes 1 and 2, respectively, are located at $\mathbf{r}_{U1}$ and $\mathbf{r}_{U2}$, the fundamental partition function Q_0 is expressed as $Q(\mathbf{r}_{U1},\mathbf{r}_{U2})$ which is written as

$$\begin{aligned} Q(\mathbf{r}_{U1},\mathbf{r}_{U2}) &= c\int\cdots\int \delta(\mathbf{r}'_{U1}-\mathbf{r}_{U1})\delta(\mathbf{r}'_{U2}-\mathbf{r}_{U2})\exp(-\beta U)d\mathbf{r}'_{U1}d\mathbf{r}'_{U2}d\mathbf{r}_1\cdots d\mathbf{r}_N \\ &= c\int\cdots\int \exp\{-\beta U(\mathbf{r}_{U1},\mathbf{r}_{U2},\mathbf{r}_1,\cdots,\mathbf{r}_N)\}\,d\mathbf{r}_1\cdots d\mathbf{r}_N, \end{aligned} \tag{A.5}$$

where c represents the coefficient of Eq. (A.1). The content of U is described as

$$U = \sum_{i\neq j} u(\mathbf{r}_j-\mathbf{r}_i) + \sum_{i=1}^{N} u_1(\mathbf{r}_i-\mathbf{r}_{U1}) + \sum_{i=1}^{N} u_2(\mathbf{r}_i-\mathbf{r}_{U2}), \tag{A.6}$$

where u, u_1, and u_2 represent the two body potentials between solvent-solvent, solvent-solute 1, and solvent-solute 2, respectively. The first summation term in Eq.

(A.6) can be expressed as

$$\sum_{i\neq j} u(\mathbf{r}_j - \mathbf{r}_i) = \frac{1}{2}\left\{\sum_i^N \sum_j^N u(\mathbf{r}_j - \mathbf{r}_i) - \sum_k^N u(\mathbf{r}_k - \mathbf{r}_k)\right\}. \tag{A.7}$$

The partition function $Q(\mathbf{r}_{U1},\mathbf{r}_{U2})$ has the hole system energy U, however, there is not two-body potential between the solutes 1 and 2 (see Eq. (A.6)). The reason of the absence is that the two-body potential between the solutes 1 and 2 does not have an influence on the solvation force. That is, the solvation force (f_{sol}) and the two-body force between the solutes (f_{12}) are independent in a classical manner, which is expressed as $f_{tot} = f_{sol} + f_{12}$ where f_{tot} is the total force between the solutes 1 and 2. (If one substitutes all of the two-body potentials into U, one can purely separate the solvation force and the two-body force between two solutes by analyzing the partition function.)

Next, the solvation force acting between the solutes 1 and 2 being $\mathbf{f}_{12}$ (i.e., solvation force acting on the solute 2 near the solute 1) is written as

$$\mathbf{f}_{12} = -\frac{\partial \Phi(\mathbf{r}_{U1}, \mathbf{r}_{U2})}{\partial \mathbf{r}_{U2}} = -\frac{\partial}{\partial \mathbf{r}_{U2}}\{F(\mathbf{r}_{U1}, \mathbf{r}_{U2}) - F(\mathbf{r}_{U1}, \infty)\}, \tag{A.8}$$

where Φ and F represent the potential of the mean force and solvent's free energy, respectively. The sign ∞ represents that the solute 2 is sufficiently (infinitely) far from the solute 1. The partial differentiation with respect to $\mathbf{r}_{U2}$ has the form:

$$\frac{\partial}{\partial \mathbf{r}_{U2}} = \frac{\partial}{\partial x_{U2}}\mathbf{i} + \frac{\partial}{\partial y_{U2}}\mathbf{j} + \frac{\partial}{\partial z_{U2}}\mathbf{k}, \tag{A.9}$$

where **i**, **j**, and **k** are unit vectors of x-, y-, and z-axes, respectively. Since $F(\mathbf{r}_{U1}, \infty)$ is the constant, the partial differentiation with respect to $\mathbf{r}_{U2}$ is *zero*. Here, applying a bridge function between thermodynamics and statistical mechanics (i.e., $F(\mathbf{r}_{U1},\mathbf{r}_{U2}) = -k_B T \ln Q(\mathbf{r}_{U1},\mathbf{r}_{U2})$), Eq. (A.8) is rewritten as

$$\mathbf{f}_{12} = -\frac{\partial}{\partial \mathbf{r}_{U2}}(-k_B T \ln Q) = k_B T \frac{1}{Q}\frac{\partial Q}{\partial \mathbf{r}_{U2}}, \tag{A.10}$$

where the partial differentiation of Q with respect to $\mathbf{r}_{U2}$ is

$$\frac{\partial Q}{\partial \mathbf{r}_{U2}} = -\beta c \int \cdots \int \left(\frac{\partial U}{\partial \mathbf{r}_{U2}}\right) \exp(-\beta U) d\mathbf{r}_1 \cdots d\mathbf{r}_N, \tag{A.11}$$

and the partial differentiation of U with respect to $\mathbf{r}_{U2}$ is

$$\frac{\partial U}{\partial \mathbf{r}_{U2}} = \frac{\partial}{\partial \mathbf{r}_{U2}} \sum_{i=1}^{N} u_2(\mathbf{r}_i - \mathbf{r}_{U2}). \tag{A.12}$$

By substituting Eq. (A.12) into Eq. (A.11), it is rewritten as

$$\begin{aligned} \frac{\partial Q}{\partial \mathbf{r}_{U2}} &= -\beta c \int \cdots \int \sum_{i=1}^{N} \left\{ \frac{\partial}{\partial \mathbf{r}_{U2}} u_2(\mathbf{r}_i - \mathbf{r}_{U2}) \right\} \exp(-\beta U) d\mathbf{r}_1 \cdots d\mathbf{r}_N \\ &= -\beta c N \int \cdots \int \left\{ \frac{\partial}{\partial \mathbf{r}_{U2}} u_2(\mathbf{r}_1 - \mathbf{r}_{U2}) \right\} \exp(-\beta U) d\mathbf{r}_1 \cdots d\mathbf{r}_N. \end{aligned} \tag{A.13}$$

By the way, the distribution of the number density (ρ) wherein the solutes 1 and 2 respectively are located at $\mathbf{r}_{U1}$ and $\mathbf{r}_{U2}$ is defined as

$$\rho(\mathbf{r}; \mathbf{r}_{U1}, \mathbf{r}_{U2}) = \langle \sum_{i=1}^{N} \delta(\mathbf{r}_i - \mathbf{r}) \rangle \tag{A.14}$$

Here, $< X >$ means an ensemble average of X with respect to the partition function $Q(\mathbf{r}_{U1},\mathbf{r}_{U2})$. Thus, Eq. (A.14) is rewritten as

$$\rho(\mathbf{r}; \mathbf{r}_{U1}, \mathbf{r}_{U2}) = \frac{Nc}{Q} \int \cdots \int \exp\{-\beta U(\mathbf{r}_{U1}, \mathbf{r}_{U2}, \mathbf{r}, \mathbf{r}_2, \cdots, \mathbf{r}_N)\} d\mathbf{r}_2 \cdots d\mathbf{r}_N, \tag{A.15}$$

and it is rewritten as following form,

$$\int \cdots \int \exp\{-\beta U(\mathbf{r}_{U1}, \mathbf{r}_{U2}, \mathbf{r}_1, \mathbf{r}_2, \cdots, \mathbf{r}_N)\} d\mathbf{r}_2 \cdots d\mathbf{r}_N = \frac{Q\rho(\mathbf{r}_1; \mathbf{r}_{U1}, \mathbf{r}_{U2})}{Nc}. \tag{A.16}$$

In Eq. (A.16), we replaced $\mathbf{r}$ with $\mathbf{r}_1$ (see Eq. (A.15)). The value of $\mathbf{r}_1$ itself is not changed from $\mathbf{r}$, i.e. only the character itself is replaced. Then, we substitute Eq. (A.16) into Eq. (A.13), and we obtain

$$\frac{\partial Q}{\partial \mathbf{r}_{U2}} = -\beta c N \int \left\{ \frac{\partial u_2(\mathbf{r}_1 - \mathbf{r}_{U2})}{\partial \mathbf{r}_{U2}} \right\} \frac{Q\rho(\mathbf{r}_1; \mathbf{r}_{U1}, \mathbf{r}_{U2})}{Nc} d\mathbf{r}_1. \tag{A.17}$$

Consequently, the solvation force is expressed as

$$\mathbf{f}_{12}(\mathbf{r}_{U1}, \mathbf{r}_{U2}) = -\int \rho(\mathbf{r}_1; \mathbf{r}_{U1}, \mathbf{r}_{U2}) \left\{ \frac{\partial u_2(\mathbf{r}_1 - \mathbf{r}_{U2})}{\partial \mathbf{r}_{U2}} \right\} d\mathbf{r}_1. \quad \text{(A.18)}$$

If the partial differentiation with respect to $\mathbf{r}_{U2}$ is replaced by that with respect to $\mathbf{r}_1$, Eq. (A.18) is rewritten as

$$\mathbf{f}_{12}(\mathbf{r}_{U1}, \mathbf{r}_{U2}) = \int \rho(\mathbf{r}_1; \mathbf{r}_{U1}, \mathbf{r}_{U2}) \left\{ \frac{\partial u_2(\mathbf{r}_1 - \mathbf{r}_{U2})}{\partial \mathbf{r}_1} \right\} d\mathbf{r}_1. \quad \text{(A.19)}$$

Eq. (A.19) is the basic relational expression between $\mathbf{f}_{12}$ and ρ. Eq. (1), the fundamental equation for deriving the transform methods 1 and 2, is derived by extracting the z-component of the solvation force.

References

[1] R. G. Horn and J. N. Israelachvili, J. Chem. Phys. **75** (1981) 1400.
[2] K. Ueno, M. Katsuya, M. Watanabe, M. Mizukami, and K. Kurihara, Phys. Chem. Chem. Phys. **12** (2010) 4066.
[3] I. K. Snook and W. van Megen, J. Chem. Soc. **77** (1981) 181.
[4] P. Tarazona and L. Vicente, Mol. Phys. **56** (1985) 557.
[5] L. J. D. Frink and F. van Swol, J. Chem. Phys. **108** (1998) 5588.
[6] H. Matsubara, F. Pichierri, and K. Kurihara, J. Chem. Phys. **134** (2011) 044536.
[7] J. G. Kirkwood, J. Chem. Phys. **10** (1942) 394.
[8] Y. Karino, R. Akiyama, and M .Kinoshita, J. Phys. Soc. Jpn. **78** (2009) 044801.
[9] Y. Kubota and R. Akiyama, J. Phys. Soc. Jpn. **81** (2012) SA017.
[10] M. Watkins and B. Reischl, J. Chem. Phys. **138** (2013) 154703.
[11] K. Amano, K. Suzuki, T. Fukuma, O. Takahashi, and H. Onishi, J. Chem. Phys. **139** (2013) 224710.
[12] J. E. Sader, T. Uchihashi, M. J. Higgins, A. Farrell, Y. Nakayama, and S. P. Jarvis, Nanotech. **16** (2005) S94.
[13] T. Fukuma, Y. Ueda, S. Yoshioka, and S. Asakawa, Phys. Rev. Lett. **104** (2010) 016101.
[14] J. P. Cleveland, T. E. Schaffer, and P. K. Hnasma, Phys. Rev. B Rappid Communications **52** (1995).
[15] J. P. Hansen and L. R. McDonald, *Theory of Simple Liquids* (Academic Press,

London, 1986).
[16] M. Kinoshita, S. Iba, and M. Harada, J. Chem. Phys. **105** (1996) 2487.
[17] R. Roth, J. Phys. Condens. Matter **22** (2010) 063102.
[18] R. Ishizuka and N. Yoshida, J. Chem. Phys. **139** (2013) 084119.
[19] D. Henderson and L. Blum, J. Chem. Phys. **75** (1978) 5441.
[20] D. Henderson and L. Blum, J. Chem. Phys. **69** (1981) 2025.
[21] P. Bryk, R. Roth, K. R. Mecke, and S. Dietrich, Phys. Rev. E **68** (2003) 031602.
[22] K. Amano and M. Kinoshita, Chem. Phys. Lett. **504**, (2011) 221.
[23] K. Amano, H. Oshima, and M. Kinoshita, J. Chem. Phys. **135** (2011) 185101.
[24] K. Amano, Physica A **391** (2012) 4615.
[25] J. N. Israelachvili, *Intermolecular and Surface Forces* (Academic Press, New York, 1991).
[26] O. Chara, A. N. MacCarthy, C. G. Ferrara, E. R. Caffarena, and J. R. Grigera, Physica A **388** (2009) 4551.
[27] F. Taherian, V. Marcon, and N. F. A. van der Vegt, Langmuir **29** (2013) 1457.
[28] K. Amano and E. Tanaka, arXiv:1408.2730 (2014).
[29] C. D. Dushkin and K. Kurihara, Coll. Surf. A **129-130** (1997) 131.
[30] P. Richetti and P. Kékicheff, Phys. Rev. Lett. **23** (1992) 1951.
[31] J. C. Crocker, J. A. Matteo, A. D. Dinsmore, and A. G. Yodh, Phys. Rev. Lett. **82** (1999) 4352.
[32] S. Nihonyanagi, S. Yamagushi, and T. Tahara, J. Chem. Phys. **130** (2009) 204704.
[33] J. A. Mondal, S. Nihonyanagi, S. Yamaguchi, and T. Tahara, J. Am. Chem. Soc. **132** (2010) 10656.

Figure and Table captions

Fig. 1. Cylindrical solids 1 and 2 are immersed in the solvent. The black point is the origin of the whole system. The black and gray points are the origin of the functions of g_1 and g_2, respectively. (g_1 and g_2 are the normalized number densities of the solvent around the isolated cylindrical solids 1 and 2, respectively. In this paper, they are simply called “solvation structure”.) The double-headed arrow represents the separation between the two circular surfaces. At first, the force acting on cylindrical solid 2 is measured. Next, the solvation structure on cylindrical solid 1 is calculated by the transforming methods.

Fig. 2. Comparisons of the solvation structures calculated by the normal method (g_n: blue solid line), the transform method 1 (g_{t1}: red dashed line), and the transform method 2 (g_{t2}: green dotted line). The solvent here is the hard sphere fluid. The values

of g_C^{n}, g_C^{t1}, and g_C^{t2} represent normalized number densities at the contact point calculated by the normal method, the transform methods 1 and 2, respectively. In (a), (b), (c), and (d), dimensionless values of the solvent number density being $\rho_0 d_S^3$ are 0.5, 0.6, 0.7, and 0.8, respectively. When $h/d_S = 0.5$, the solvent sphere contacts the circular surface, i.e. it is the contact point. The parts of the lines calculated by the transform method 2 are not displayed due to the large deviation.

Fig. 3. Comparisons of the solvation structures calculated by the normal method (g_n: blue solid line), the transform method 1 (g_{t1}: red dashed line), and the transform method 2 (g_{t2}: green dotted line). The solvent here is the LJ fluid with hard core potential. In (a)-(c), dimensionless values of the solvent number density being $\rho_0 d_S^3$ is 0.7 and affinity between the two solvent spheres being $\xi_{SS}/(k_B T)$ is 1.5. The values of g_C^{n}, g_C^{t1}, and g_C^{t2} represent normalized number densities at the contact point calculated by the normal method, the transform methods 1 and 2, respectively. In (a), (b), and (c), the solvation affinity of the cylindrical solid being $\xi_{DS}/(k_B T)$ is set at 0.0 (solvophobic), 1.0 (neutral), and 2.0 (solvophilic), respectively. When $h/d_S = 0.5$, the solvent sphere contacts the circular surface, i.e. it is the contact point. The parts of the lines calculated by the transform method 2 are not displayed due to the large deviation.

Table 1. Surface area of the deviation (S_{dev}) in the hard sphere fluid. The values are calculated by using Eq. (17).

Table 2. Surface area of the deviation (S_{dev}) in the LJ fluid. The values are calculated by using Eq. (17). The values of $\rho_0 d_S^3$ and $\xi_{SS}/(k_B T)$ are set at 0.7 and 1.5, respectively.

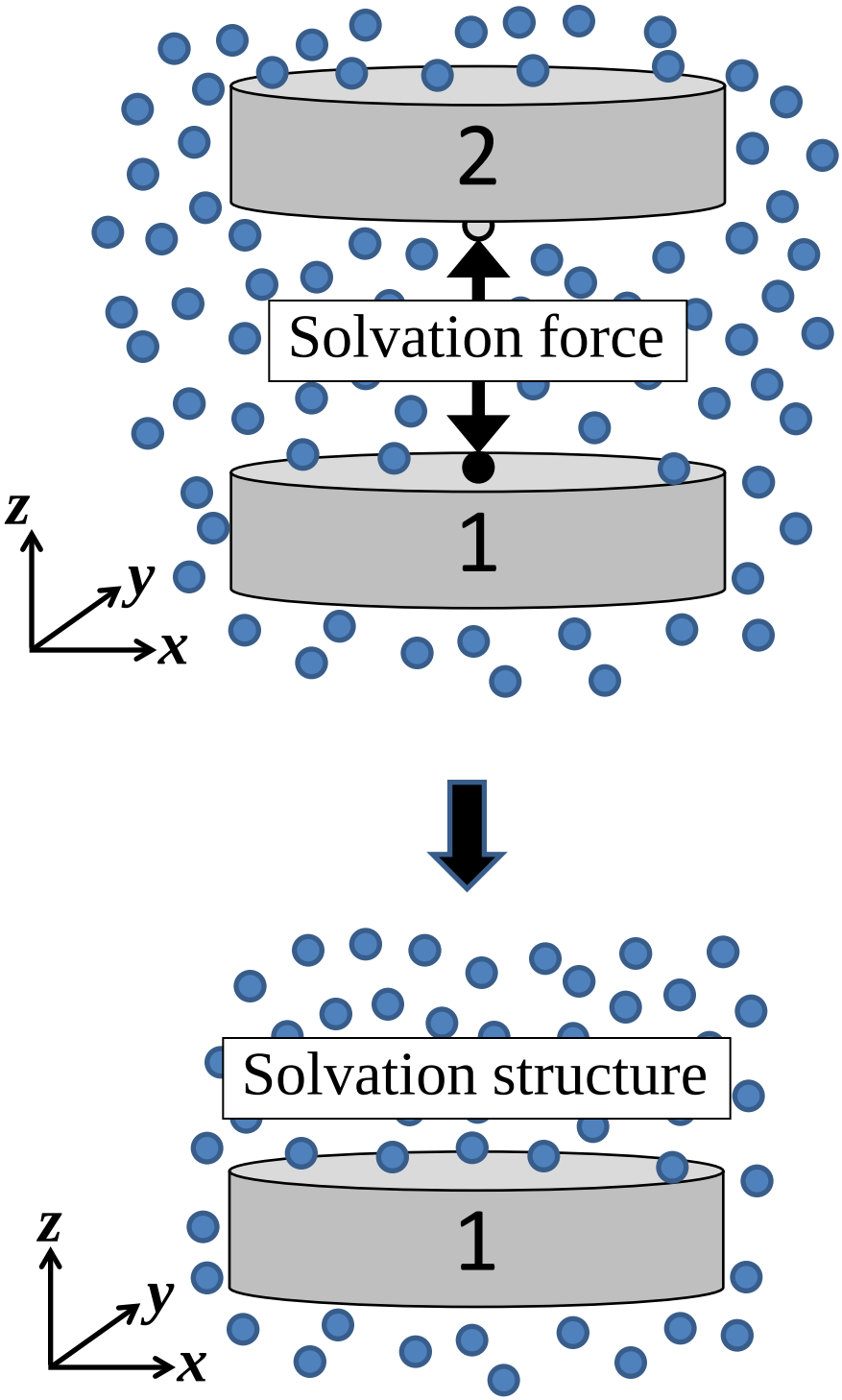

Fig. 1

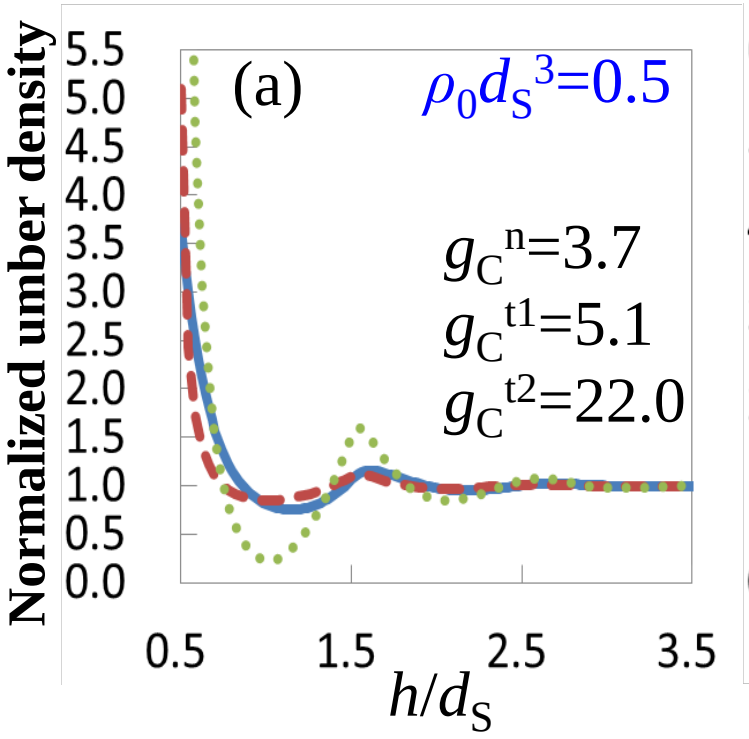

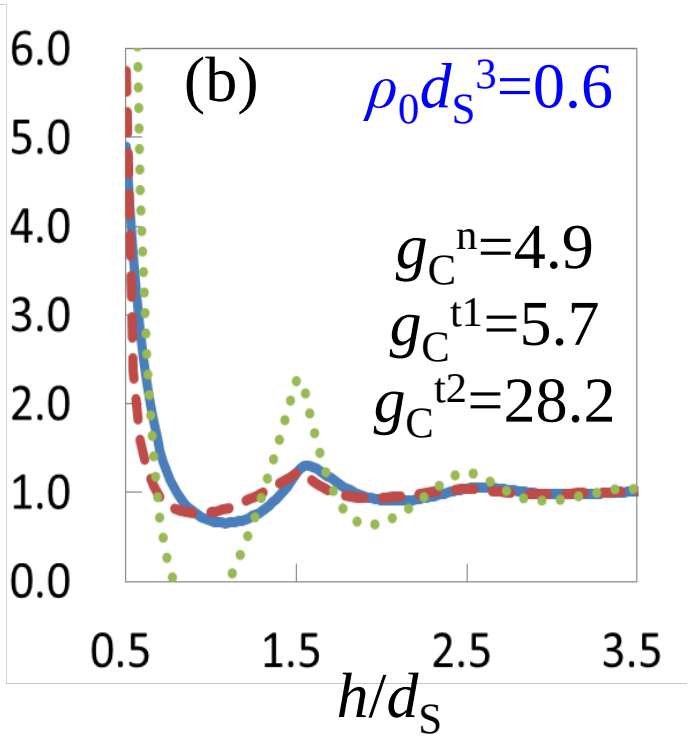

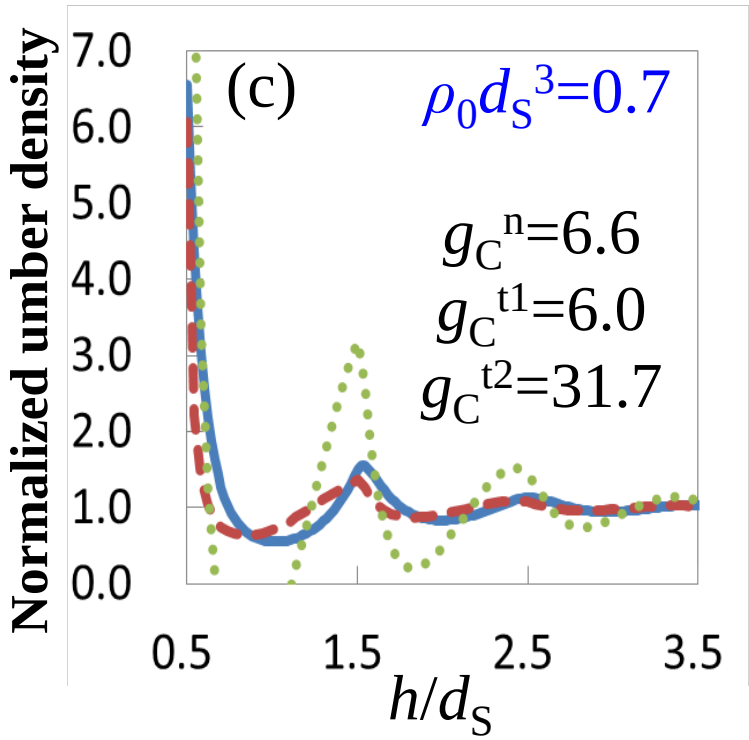

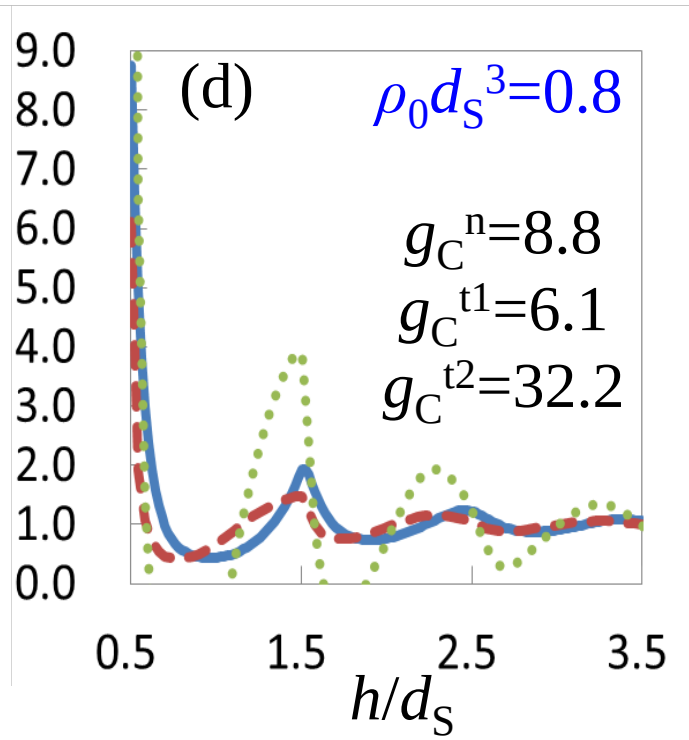

Fig. 2

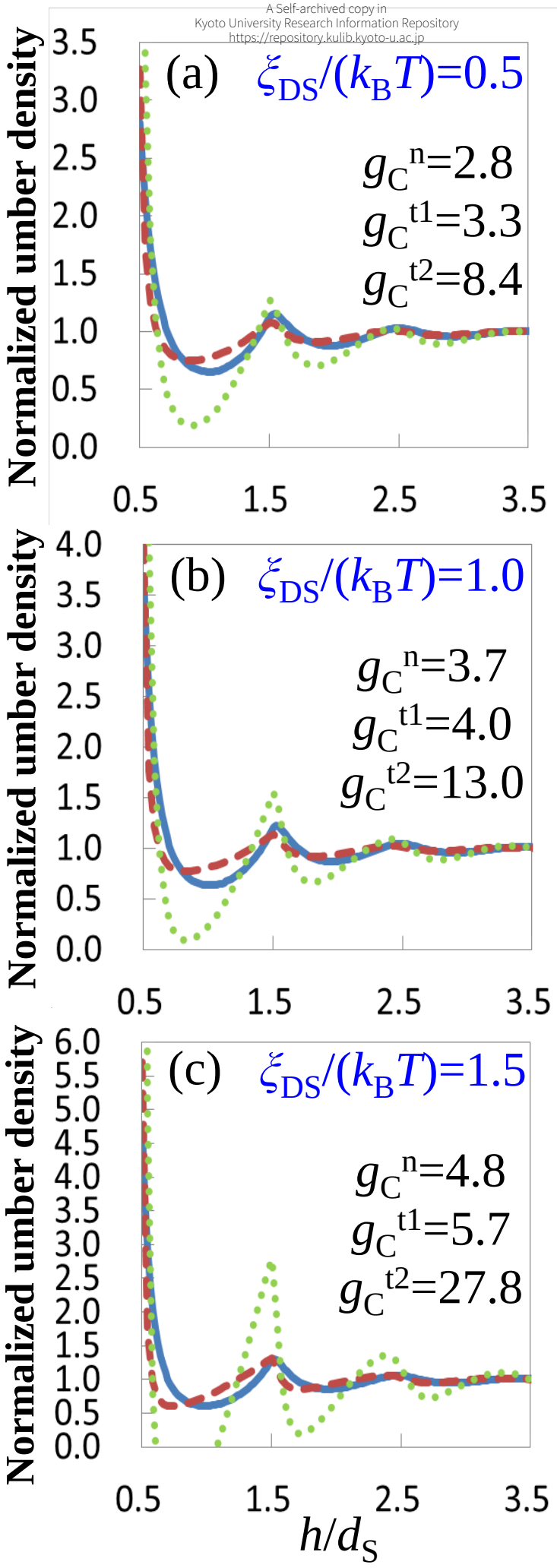

Fig. 3

$\rho_0 {d_S}^3$	Kirkwood (g_{t1})	Linear (g_{t2})
0.5	0.31	1.52
0.6	0.42	2.12
0.7	0.56	2.87
0.8	0.88	3.90

Table 1

$\zeta_{DS}/(k_B T)$	Kirkwood (g_{t1})	Linear (g_{t2})
0.5	0.21	0.69
1.0	0.28	0.93
1.5	0.43	2.61

Table 2